ACS APPLIED BIO MATERIALS Cite This: ACS Appl. Bio Mater. XXXX, XXX, XXX−XXX

Article

www.acsabm.org

Click-Engineered, Bioresponsive, and Versatile Particle−Protein−Dye System

Mary K. Burdette,[†,‡] Ragini Jenkins,[†,‡] Yuriy P. Bandera,[†,‡] Haley Jones,[†,‡] Isabell K. Foulger,[¶,‡] Ashley Dickey,[‡,§] Anna-Liisa Nieminen,[⊥] and Stephen H. Foulger*[,†,‡,¶]

[†]Department of Materials Science and Engineering, Advanced Materials Research Laboratories, [‡]Center for Optical Materials Science and Engineering Technologies, Advanced Materials Research Laboratories, and [§]Department of Chemistry, Advanced Materials Research Laboratories, Clemson University, Anderson, South Carolina 29625, United States

[⊥]Drug Discovery & Biomedical Sciences, Medical University of South Carolina, Charleston, South Carolina 29425, United States

[¶]Department of Bioengineering, Clemson University, Clemson, South Carolina 29634, United States

ABSTRACT: We present a multifunctional polymer based nanoparticle platform for personalized nanotheranostic applications, which include photodynamic therapy and active targeting. In this system, poly(propargyl acrylate) (PA) particles were surface-modified with organic ligands and fluorophores (the payload) through an environmentally-sensitive linker. An azide modified bovine serum albumin (azBSA) was employed as the linker. This system prevents opsonization and, upon digestion, releases the payload. Attachment of the emitting payload to the particle through azide-modified bovine serum albumin (BSA) quenches emission, which can be again activated with digestion of the azBSA. The emission "turn-on" at a specific location will increase the signal-to-noise ratio. By utilizing human head and neck squamous carcinoma cells (UMSCC22A), photodynamic therapy studies with these particles gave promising reductions in cell growth. Additionally, the particle−protein−dye system is versatile as different fluorophores (such as silicon phthalocyanine or cyanine 3) can be attached to the protein and the same activation/deactivation behavior is observed. Active targeting can be employed to enhance the concentration of the payload in the designated tumor. Human lung carcinoma cells (A549) were utilized in toxicity studies where PA-azBSA particles were modified with a Survivin targeting ligand and indicated an enhanced cell death with the modified particles relative to the "free" Survivin targeting ligand.

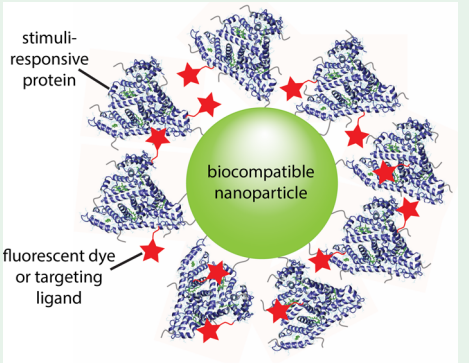

KEYWORDS: *photodynamic therapy, active targeting, multifunctional, bioresponsive, protein/nanoparticle conjugate*

1. INTRODUCTION

Recently there has been significant effort on the development of multifunctional nanocarriers such as biodegradable polymeric nanoparticles,[1,2] dendrimers,[3] magnetic and other metal particles,[4,5] surface cross-linked micelles,[6,7] and liposomes[4] for cancer theranostics. Among these differing technologies, systems that are based on polymeric materials, specifically nanoparticles that are biodegradable, have gained immense interest due to their inherent tailorability in macromolecular synthesis methods, improved drug solubility, high drug loading capacities, and simplicity of multifunctionalization.[8−10] Combining imaging and therapeutic agents into a single theranostic formulation allows for the immediate identification of pharmacokinetics and provides some clarity of the relationship between patients and their tumors. This insight can be helpful for a physician to decide or change the dosage, drug choice, and treatment method accordingly and results in an effective "personalized medicine" treatment of the disease.[11] For personalized medicine treatment to be successful, a single nanocarrier should demonstrate the following properties: (1) be biocompatible/biodegradable; (2) have prolonged circulation lifetimes; (3) have the ability to accumulate in a designated zone of interest; (4) respond to stimuli, such as temperature variations, or pH, in local envoriments; (5) be an potent intracellular drug delivery system; and (6) employ real-time observation through a reporter moiety.[8,12] In creating a multifunctional nanocarrier with these properties, all functional moieties need to be located at the nanocarrier's surface to prevent opsonization, facilitate formation of beneficial host/guest assemblies, and specifically target tumors.[5,12,13]

A prevalent and quickly developing technique to prepare and surface functionalize the nanoparticles is through a copper(I) catalyzed alkyne/azide cycloaddition (CuAAC) reaction because these reactions are reliable, experimentally simple, facilitate bioconjugation, and yield products of high orthogonality and functionalization.[1,14,15] Previously, we have reported a poly(propargyl acrylate) particle surface functionalized with a near-infrared fluorophore for fluorescence imaging and photo-

Received: January 11, 2019
Accepted: July 2, 2019
Published: July 2, 2019

DOI: 10.1021/acsabm.9b00025
ACS Appl. Bio Mater. XXXX, XXX, XXX−XXX

dynamic therapy applications.[16,17] These particles exhibit a good tumor-to-background ratio and have good circulation lifetimes, but attaching the fluorophore directly to the particle resulted in a decrease in the emission of the system. In addition, the contrast agents are attached to the particles at all times, which make it less attractive for drug delivery applications. To this end, we need to design an improved system of surface modified particles, particularly, a system that is stimuli responsive to biological factors. Bovine serum albumin (BSA) was chosen as the linker because it is stable, inert to many biochemical reactions, and prevents nonspecific adsorption of other proteins to surfaces.[18]

Recently, the quantification and digestion of bovine serum albumin (BSA) covalently conjugated to gold nanoparticles were illustrated, and in these particles, the protein was conjugated to the surface of the particles using a standard NHS activation approach, where the primary amines of the protein reacted with carboxyl containing substrates and formed a covalent amide bond.[18] This conjugation with NHS substrates is a well-established strategy and is widely used to construct fluorescent oligonucleotides and proteins.[19,20] By utilizing the NHS activation and CuAAC reactions, the improved system of modified particles can be made. In this current effort, we present a particle−protein−dye system (cf. Figure 6), where the particles are surface modified with the azide modified BSA (azBSA) that is conjugated to fluorophores. These fluorophore-functionalized particles exhibit improved efficiencies in imaging and photodynamic therapy applications because they are activated only after the digestion of the azBSA protein. This allows the particles to be in the "off" state until they reach their end locations, which is the lysosome and endosome.[16] The endosomes and lysosomes contain digestive enzymes resulting in the digestion of the albumin linker, which releases the fluorophore and results in an emission activation. In addition, this system can also be prepared such that a ligand is attached instead of the fluorophore to use it for targeting and other delivery applications, and if desired, the azBSA can be conjugated with a number of fluorophores, ligands, antibodies, and drugs at the same time by adjusting the ratios of those small molecules during CuAAC reactions. These multiple functionalized particles represent a single "nanodevice" that can be a very attractive platform for personalized medicine.

2. EXPERIMENTAL SECTION

2.1. Reagents and Solvents. All commercial reagents were used without further purification and dried according to standard methods. Deionized (DI) water was obtained from a Nanopure System and exhibited a resistivity of ~10^{18} ohm^{-1} cm^{-1}. 5-Iodopent-1-yne was synthesized from procedures in the literature.[21]

2.2. Characterization. A JEOL ECX-300 spectrometer (300 MHz for proton and 76 MHz for carbon) was used for the ^{1}H and ^{13}C NMR spectra. Chemical shifts for carbons are reported in parts per million downfield from tetramethylsilane (TMS) and are referenced to the carbon resonances of the solvent ($CDCl_3$, δ 77.16; DMSO-d6, δ 39.52 ppm), while the chemical shifts for protons are reported in parts per million downfield from TMS and are referenced to residual protium in the NMR solvent ($CDCl_3$, δ 7.26 ppm; DMSO-d6, δ 2.50 ppm). Denaturation data of the proteins from thermal cycling were obtained with a Nano DSC (microcalorimeter) provided by TA Instruments. A Shimadzu GC-17A mass spectrometer was used for electron impact (EI) (70 eV) ionization mass spectra. A Finnigan LCQ spectrometer and HP 1100 (high-performance liquid chromatography, HPLC) were employed for the LC−MS mass spectra.

2.3. Syntheses. *2.3.1. 2,5-Dioxopyrrolidin-1-yl 3-azidopropanoate (azNHS, 1).* 2-Azidopropyonic acid (1.8 g, 15.64 mmol) and *N*-hydroxysuccinimide (1.98 g, 17.2 mmol) were dissolved in THF (30 mL). The solution obtained was cooled with ice, and *N*,*N*′-dicyclohexylcarbodiimide (3.54 g, 17.2 mmol) was added. The mixture was stirred at 0 °C for half an hour followed by stirring for 6 h at room temperature. The solution was then filtered, while the insoluble solid was washed with dichloromethane. The filtrates were combined and evaporated, and the residue was dissolved in dichloromethane (15 mL), cooled in the freezer, and filtered to remove the precipitates. The filtrate was evaporated, while the product was used without additional purification[22] (cf. Figure 1). Yield 3.3 g (99%), clear oil. ^{1}H NMR ($CDCl_3$) δ 2.86 (s, 4H), 2.89 (t, 2H, J = 6.5 Hz), 3.69 (t, 2H, J = 6.5 Hz).

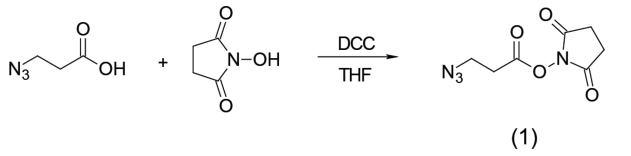

Figure 1. Reaction scheme for synthesis of azNHS.

2.3.2. Modification of BSA. Bovine serum albumin (BSA) is a 67 kDa single polypeptide consisting of 59 lysine residues. *N*-Hydroxysuccinimide (NHS) esters are commonly used to cross-link or label peptides and proteins since their primary amines can react with NHS esters in physiologic to slightly alkaline conditions to yield stable amide bonds. In the current system, BSA was modified to have free azide end groups. Standard NHS coupling reactions were used to label the protein with azido groups.[19] Briefly, BSA was reacted with an excess of azide modified *N*-hydroxysuccinimide ester (azNHS) to produce azide-labeled BSA (azBSA). The product was dialyzed in a 12−14k MWCO dialysis bag for 2 days to remove excess reactants. Unmodified BSA is a prolate ellipsoid with hydrodynamic dimensions of 14 × 4 × 4 nm^3.[23]

The azide-modified BSA (azBSA) exhibited no toxicity to HEK-293 (human embryonic kidney) cells. Figure 2 presents the cell viability of HEK cells incubated for 18 h at concentrations of "free" (unattached to particles) azBSA of 5 × 10^{-3} μM, 5 × 10^{-2} μM, 5 × 10^{-1} μM, and 5.0 μM.

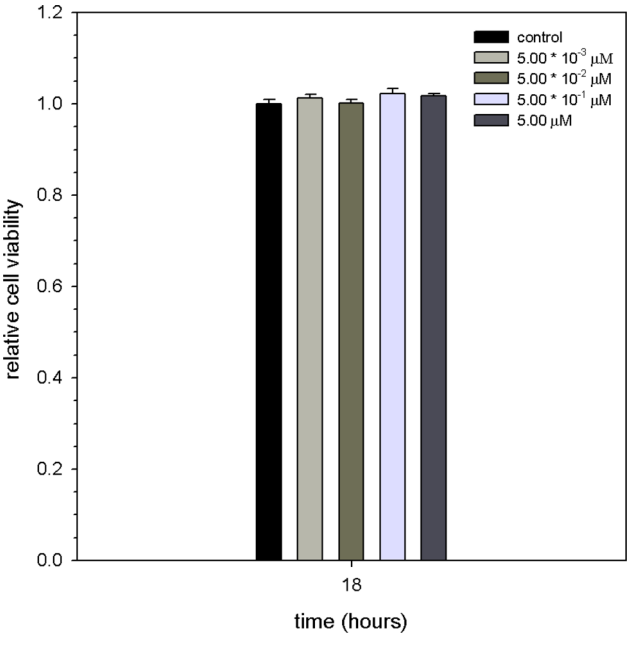

Figure 2. Cell viability of "free" azBSA in HEK-293 cells.

DOI: 10.1021/acsabm.9b00025
ACS Appl. Bio Mater. XXXX, XXX, XXX−XXX

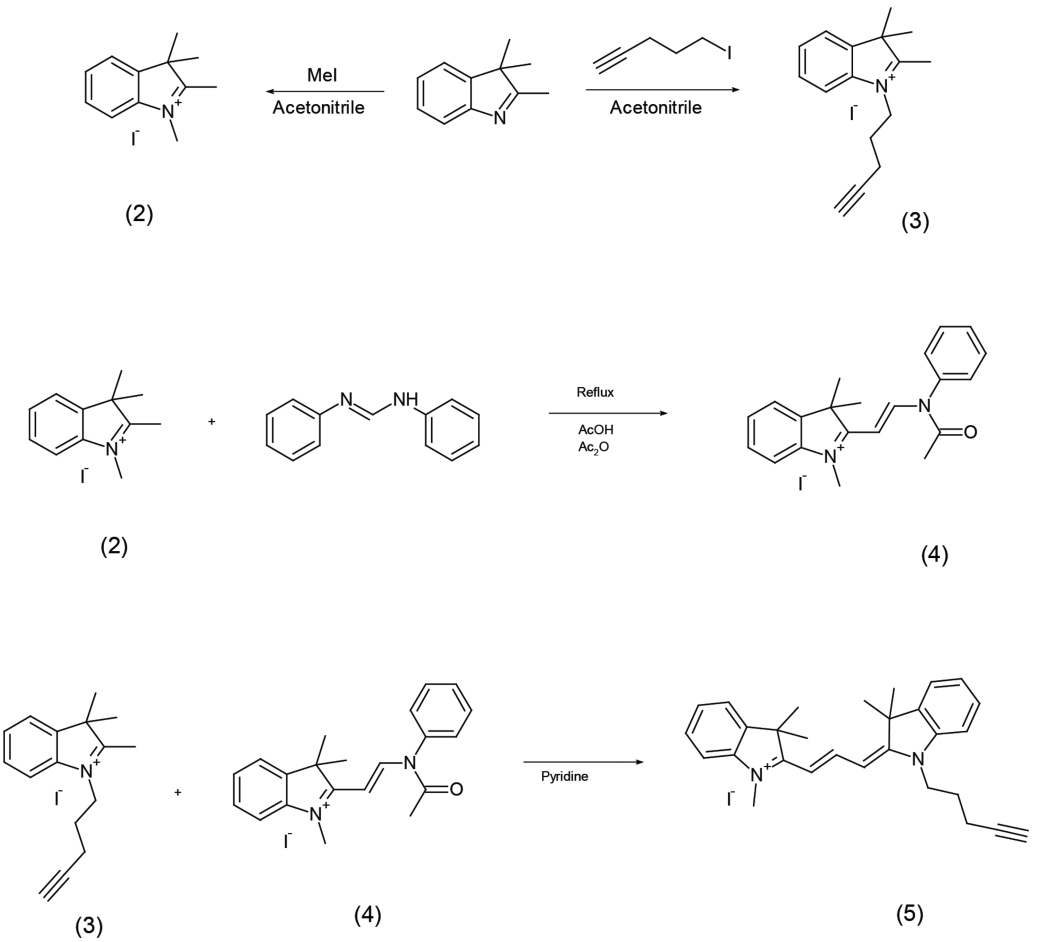

Figure 3. Reaction scheme for synthesis of alCYN.

*2.3.3. 1,2,3,3-Tetramethyl-3H-indolium iodide (**2**).* 1,2,3,3-Tetramethyl-3H-indolium iodide was synthesized according to the literature.[24] Specifically, 2,3,3-trimethyl-3H-indole (0.5 g, 3.14 mmol) and iodomethane (1.34 g, 9.42 mmol) were dissolved in acetonitrile (5 mL) and then refluxed for 5 h. The solution was then cooled to room temperature, and the solid precipitate was filtered, washed with acetone, and then dried under vacuum to yield a white crystalline product. Yield 0.94 g (99%), mp = 259 °C (lit). ^{1}H NMR (DMSO-d6) δ 1.53 (s, 6H), 2.76 (s, 3H), 3.97 (s, 3H), 7.60−7.64 (m, 2H), 7.81−7.84 (m, 1H), 7.90−7.93 (m, 1H).

*2.3.4. 2,3,3-Trimethyl-1-pent-4-ynyl-3H-indolium iodide (**3**).* 2,3,3-Trimethyl-3H-indole (0.83 g, 5.21 mmol) mixed with 5-iodo-pent-1-yne (1.5 g, 7.82 mmol) in acetonitrile (10 mL) was refluxed for 24 h. After cooled to room temperature, the solvent was evaporated. The brown residue was then crystallized with acetone. The obtained solid was filtered, washed with acetone, and dried under vacuum. Yield 1.05 g (57%), mp = 190 °C. ^{1}H NMR (DMSO-d6) δ 1.54 (s, 6H), 2.06 (m, 2H, J = 7.4 Hz), 2.42 (m, 2H, J = 7.4 Hz, J = 2.6 Hz), 2.84 (s, 3H), 2.96 (t, 1H, J = 2.6 Hz), 4.92 (t, 2H, J = 7.4 Hz), 7.63 (m, 2H), 7.85 (m, 1H), 7.96 (m, 1H).

*2.3.5. 2-[2-(Acetyl-phenyl-amino)-vinyl]-1,3,3-trimethyl-3H-indolium iodide (**4**).* 1,2,3,3-Tetramethyl-3H-indolium iodide (**2**) (0.65 g, 2.16 mmol) and *N*,*N*′-diphenyl-formamidine (0.51 g, 2.60 mmol) were mixed with acetic anhydride (4 mL) and acetic acid (8 mL), refluxed, and stirred for 1 h. After cooling, the solvent was evaporated, and the residue was dissolved in dichloromethane (2 mL). This solution was then combined with a diethyl ether solution. The resulting precipitated dark solid was separated through centrifugation. This crude product was dissolved in dichloromethane and washed with deionized (DI) water. The organic layer was separated and evaporated, with the obtained residue being dissolved in dichloromethane and then precipitated in diethyl ether. The dark-brown solid was filtered and dried under vacuum (cf. Figure 3). Yield 0.87 g (90%), solid, mp = 228 °C. ^{1}H NMR ($CDCl_3$) δ 1.83 (s, 6H), 2.11 (s, 3H), 3.85 (s, 3H), 5.59 (d, 1H, J = 14.3 Hz), 7.46−7.50 (m, 4H, J = 5.2 Hz, J = 1.4 Hz), 7.53−7.55 (m, 2H, J = 5.2 Hz, J = 1.4 Hz), 7.63−7.73 (m, 3H, J = 7.4 Hz, J = 1.4 Hz), 9.17 (d, 1H, J = 14.3 Hz).

*2.3.6. 2-[3-(3,3-Dimethyl-1-pent-4-ynyl-1,3-dihydro-indol-2-yli-dene)-propenyl]-1,3,3-trimethyl-3H-indolium iodide (**5**, alCYN).* Pyridine (6 mL) was used to dissolve compounds (**3**) and (**4**) and then stirred at 45 °C for 3 h. After being cooled to room temperature, the solution was added dropwise to a diethyl ether solution. The precipitate was a dark-brown crude product, which was then separated by centrifugation. The organic solution was decanted, and the obtained residue was dissolved in dichloromethane and washed with DI water. By separating the organic layer, it was then concentrated. The product was precipitated from diethyl ether solution twice more, filtered, and dried under vacuum. Yield was 0.12 g (50%), brown solid, mp = 211−213 °C with destruction. ^{1}H NMR ($CDCl_3$) δ 1.70 (s, 12H), 2.08 (t, 1H, J = 2.5 Hz), 2.11 (m, 2H, J = 6.6 Hz, J = 7.7 Hz), 2.62 (m, 2H, J = 6.6 Hz, J = 2.5 Hz), 3.80 (s, 3H), 4.40 (t, 2H, J = 7.7 Hz), 7.11−7.54 (m, 10H), 8.43 (t, 1H, J = 13.5 Hz); ^{1}3C NMR ($CDCl_3$) δ 16.51, 26.22, 28.20, 28.29, 32.94, 43.67, 48.90, 69.81, 83.65, 104.96, 105.44, 110.92, 111.04, 122.13, 122.19, 125.36, 125.42, 128.98, 129.04, 140.60, 142.27, 142.79, 150.95; ESI-Mass (m/z): calculated for $C_{29}H_{33}N_2$ $[M - I]^+$ 409.26, found 409.27.

2.3.7. Preparation of azBSA/alCYN Conjugate. To the cleaned azBSA, alCYN was attached through a CuAAC reaction that was performed in DI water.[20] The reaction continued for 24 h with stirring in the dark at a temperature of 28 °C. At the end of 24 h, the reaction was quenched by the removal of the unreacted sodium ascorbate and Cu_2SO_4 through dialysis for 48−72 h in DI water. It was found that there were 23 alCYN molecules per BSA protein. This was calculated using a previously reported method and was based on a

DOI: 10.1021/acsabm.9b00025
ACS Appl. Bio Mater. XXXX, XXX, XXX−XXX

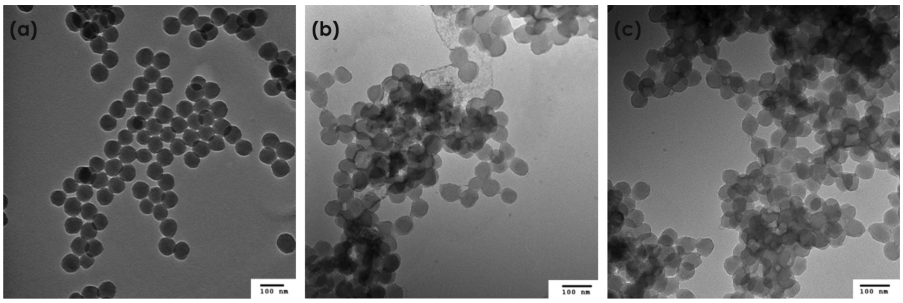

Figure 4. TEM micrographs of (a) unmodified PA particles, (b) PA particles modified with PA/azBSA, and (c) particles surface modified with albumin/cyanine 3 derivative fluorophore (PA/azBSA/alCYN). All scale bars represent 100 nm.

click reaction that involved only azBSA and alCYN with the same molecular ratios with an absence of particles.[25]

2.3.8. Preparation of Particles. Poly(propargyl acrylate) (PA) particles were synthesized following a published method.[26] Briefly, a standard aqueous emulsion polymerization technique, with a surfactant of sodium dodecyl sulfate, initiator of potassium persulfate, and cross-linker of divinylbenzene, was employed, which resulted in particles with a diameter of 88 ± 4 nm (average and standard deviation). Particle size was measured with a Coulter N4 Dynamic Light Scatterer.

2.3.9. Preparation of PA/azBSA/alCYN Particles. The cleaned azBSA/alCYN conjugate was subsequently utilized in a secondary CuAAC reaction with poly(propargyl acrylate) (PA) nanoparticles. This reaction proceeded for 48 h. The particles were then dialyzed to remove any unreacted species for 48−72 h. After dialysis, a repeated washing procedure consisting of centrifugation and redispersement in 1× phosphate buffered saline (PBS) that contained 10−30% THF by volume was performed. The last two washes were performed using only PBS, and the cleaned particles were dispersed in fresh PBS. The absorbance of the supernatant and thin layer chromatography (TLC) of the modified particles were used to confirm that all free, unbound dye was removed. TEM images were taken of the particles prior to and subsequently after modification (cf. Figure 4). The initial unmodified particles are monodisperse, and the outline of the spheres can be clearly seen. After the CuAAC reaction, the PA/azBSA/alCYN particles appeared to be wrapped together with azBSA, though it is speculated that this is due to the protein's affinity to engulf the particles during TEM sample preparation. The azBSA has multiple free azide groups before the secondary CuAAC reaction, so it is possible to attach one azBSA to two or more particles. This would result in some particles being bound together by their mutual attachment to a shared azBSA. Nonetheless, the modification of the particles with azBSA was performed under dilute conditions, and the opportunity for an azBSA to have a multiple attached particles should be infrequent.

*2.3.10. 4-(Prop-2-yn-1-yloxy)benzaldehyde (**6**).* P-Hydroxybenzaldehyde (0.3 g, 2.45 mmol) and propargyl bromide (0.38 g, 3.19 mmol) were dissolved in acetone (20 mL), and then potassium carbonate (0.34 g, 2.46 mmol) was added. The obtained mixture was stirred under reflux for 12 h. After cooling, the mixture was quenched with cold DI water and extracted with dichloromethane. The organic solution was washed with DI water, separated, dried with Na_2SO_4, filtered, and evaporated under reduced pressure. Yield 0.32 g (82%). Clear crystals, mp = 73−74 °C. ^{1}H NMR ($CDCl_3$) δ 2.57 (t, 1H, J = 2.4 Hz), 2.77 (d, 2H, J = 2.4 Hz), 7.08 (d, 2H, J = 8.9 Hz), 7.85 (d, 2H, J = 8.9 Hz), 9.89 (s, 1H).

*2.3.11. 6-(5-Chloro-2-hydroxyphenyl)-2-oxo-4-(4-(prop-2-yn-1-yloxy)phenyl)-1,2-dihydropyridine-3-carbonitrile (s102, **7**).*[27−29] 1-(5-Chloro-2-hydroxyphenyl)ethanone (0.266 g, 1.56 mmol) and 4-(prop-2-yn-1-yloxy)benzaldehyde (**6**) (0.3 g, 1.87 mmol) were dissolved in dry ethanol (7 mL). Ethyl cyanoacetate (0.23 g, 2.03 mmol) and ammonium acetate (0.72 g, 9.36 mmol) were added into the solution.[27−29] The mixture was stirred in a sealed pressure vessel for 2 h at 110 °C. After cooling, the precipitated solid was filtered, washed with cold ethanol and DI water, dried, and purified by flash column chromatography on silica with an eluent of ethyl acetate (cf. Figure 5). R_f = 0.9. Yield 0.09 g (15%), mp = 229 °C. ^{1}H NMR

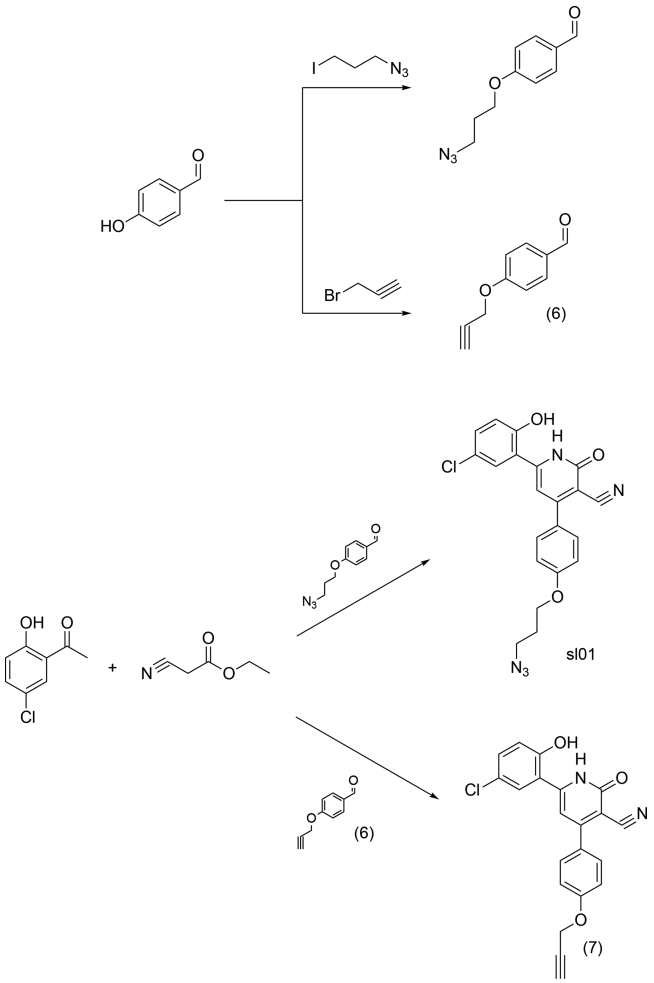

Figure 5. Reaction scheme for synthesis of alkyne modified Abbott17 derivative (s102, **7**).

(DMSO-d6) δ 3.64 (t, 1H, J = 2.2 Hz), 4.92 (d, 2H, J = 2.2 Hz), 7.13 (d, 2H, J = 8.9 Hz), 7.42 (d, 1H, J = 8.9 Hz), 7.66 (d.d, 1H, J = 8.6 Hz, J = 2.4 Hz), 7.91 (br.s, 1H), 8.01 (s, 1H), 8.33 (d, 2H, J = 8.6 Hz), 8.71 (d, 1H, J = 2.4 Hz); ^{13}C NMR (DMSO-d6) δ 55.59, 78.58, 79.05, 95.40, 100.41, 114.78, 118.72, 119.03, 124.68, 129.05, 129.18, 130.37, 130.64, 132.03, 143.48, 150.62, 158.30, 159.18, 160.18, 160.59, 160.64; ESI-Mass (m/z): calculated for $C_{21}H_{13}ClN_2O_3$ $[M + H]^+$ 377.07, found 377.07.

2.4. Optical Characterization Methods. Absorbance spectra were obtained using a PerkinElmer Lambda 900 UV−vis/NIR

DOI: 10.1021/acsabm.9b00025
ACS Appl. Bio Mater. XXXX, XXX, XXX−XXX

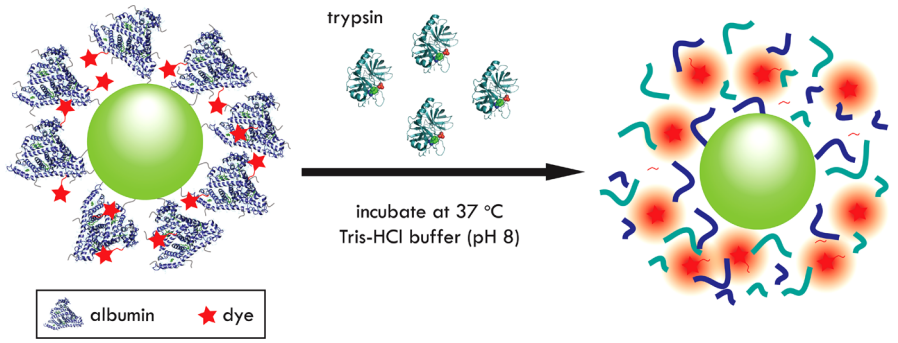

Figure 6. Schematic of the release of fluorophore from functionalized particles through trypsin digestion of the albumin. Sub 100 nm poly(propargyl acrylate) (PA) particles were surface modified with azide modified bovine serum albumin (azBSA) and alkyne terminated silicon phthalocyanine derivative (alSiPc), alkyne modified cyanine 3 (alCYN), or Abbott17 (s102) through an aqueous phase CuAAC reaction. This yielded a nanoparticle surface modified with a shell of dye or targeting ligand functionalized BSA. This intact particle−protein−dye system is not fluorescent. However, upon the addition of trypsin, a digestive enzyme, the BSA is digested into its smaller peptides, and the fluorophore is released. Upon release, the fluorophore becomes fluorescent.

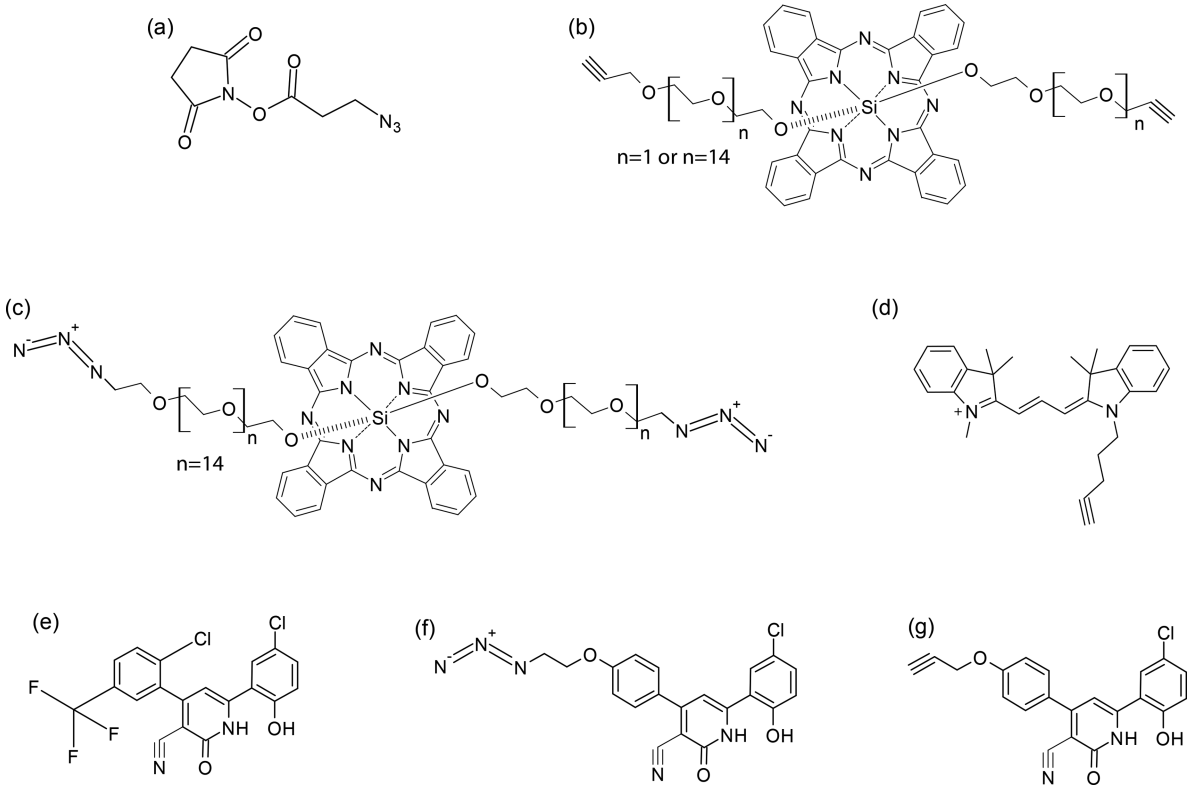

Figure 7. Structures of (a) azide modified *N*-hydroxysuccinimide derivative (azNHS), (b) alkyne modified silicon phthalocyanine fluorophore with short PEG chains (n = 1, SiPc1) and long PEG chains (n = 14, alSiPc2), (c) azide modified silicon phthalocyanine fluorophore with long PEG chains (n = 14, azSiPc), (d) alkyne modified cyanine 3 (alCYN) dye, (e) Abbott 17, (f) azide modified survivin ligand (s101), and (g) alkyne modified survivin ligand (s102).

spectrophotometer. A Thermo Oriel xenon arc lamp (Thermo Oriel 66902) coupled to a Thermo Oriel Cornerstone 7400 1/8m monochromator (Thermo Oriel 7400) and a Horiba Jobin-Yvon MicroHR spectrometer coupled to a Synapse CCD detector were employed to obtain photoluminescence (PL) spectra.

2.4.1. Cell Analysis. Human A549 cell lines were obtained from ATCC (Rockville, MD) and were cultured in F-12K media (Kaighn's Modification of Ham's F-12 medium). This media contained 1% penicillin−streptomycin and 10% fetal bovine serum (FBS). Head and neck squamous carcinoma cell line (Human UMSCC22A) was obtained from Dr. Besim Ogretmen (Medical University of South Carolina) and was cultured in Dulbecco's modified Eagle's medium (DMEM) supplemented with L-glutamine containing 1% penicillin−streptomycin and 10% FBS. Cells were cultured at 37 °C in a humidified atmosphere of 95% air, 5% CO_2. HEK-293 cells were cultured in DMEM (Dulbecco's modified Eagle's medium) containing 10% fetal bovine serum (FBS) and 1% L-glutamine. A 37 °C humidified atmosphere of 95% air 5% CO_2 was used to culture the cells. MTS (3-(4,5-dimethylthiazol-2-yl)-5-(3-carboxymethoxyphenyl)-2-(4-sulfophenyl)-2H-tetrazolium salt) assay was employed to measure cell death and used according to the manufacturer's instructions (Promega, Madison, WI). Ninety-six-well cell plates were used with 5000 cells/well.

2.4.2. Photodynamic Therapy. For 18 h, cell cultures were incubated with various concentrations of the sample before being exposed to 200−400 mJ/cm^2 red light (670 nm) from an Intense-

DOI: 10.1021/acsabm.9b00025
ACS Appl. Bio Mater. XXXX, XXX, XXX−XXX

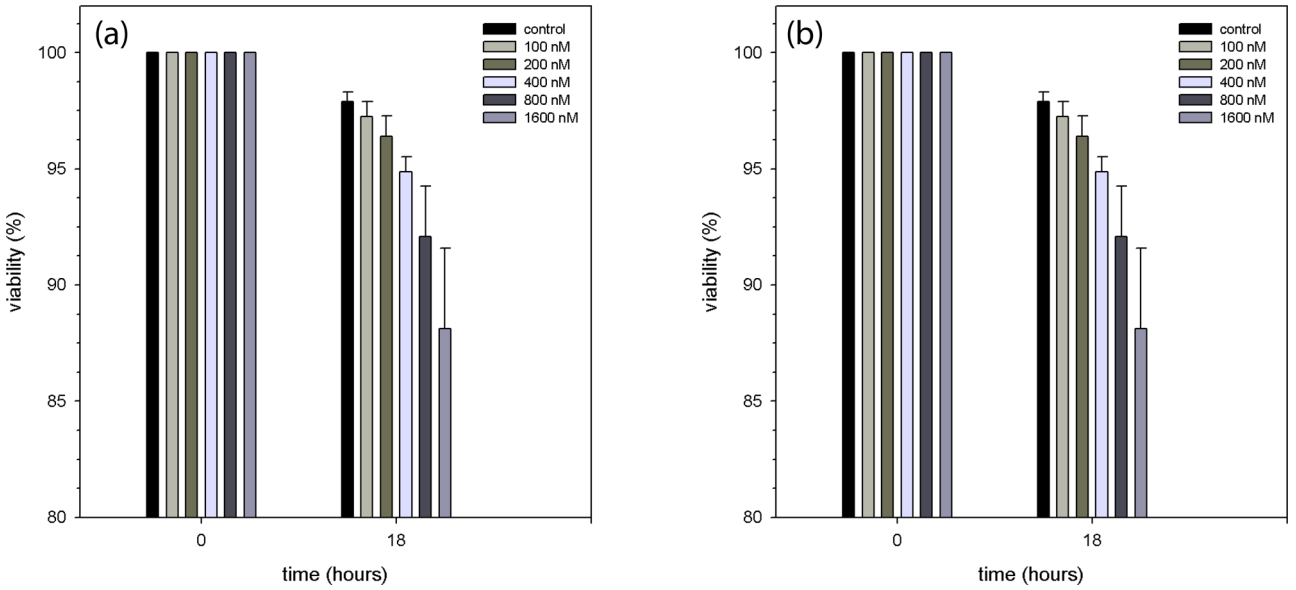

Figure 8. Cell viability of UMSCC22A (head and neck squamous carcinoma) cells incubated with surface modified particles with photodynamic therapy. (a) Cells were treated with varying concentrations of PA/azSiPc for 18 h. (b) Cells were treated with varying concentrations of PA/azBSA/alSiPc2 for 18 h. Cell viability is presented as percentage of viable cells in total population. Particles incubated with the cells.

HPD 7404 diode laser (North Brunswick, NJ). After exposure to red light, cells were incubated for various periods of time prior to analysis. As previously described,[30] cell death was assessed by propidium iodide (PI) fluorometry using a multiwell fluorescence plate reader. Cells were changed to fresh medium supplemented with PI (30 μM) and Insulin-Transferrin-Selenium-X (ITX) reagent (insulin (10 μg/mL), selenium (6.7 ng/mL), transferrin (5.5 μg/mL), ethanolamine (0.2 mg/mL)) (Gibco) but omitting FBS before exposure to light. PI fluorescence was measured at various intervals using 530 nm excitation (25 nm band-pass) and 620 nm emission (40 nm band-pass) filters. Microliter plates were placed in a 37 °C incubator between measurements. At the end of the experiment, digitonin (200 μM) was added to each well to label all nuclei with PI and permeabilize all cells. Cell viability determined by PI fluorometry was approximately the same as cell viability found through trypan blue exclusion.[30]

2.4.3. Cytotoxicity Assay. A549 cells or HEK-293 (5000 cells per well) were cultured on 96-well plates for 24 h. Subsequently, A549 cells were exposed to 1, 2.5, 5, 10, 15, and 20 μM PA-azBSA-s102, 20 μM PA, and 1, 2.5, 5, 10, 15, and 20 μM s101. After 48 h, cell death was assessed with a MTS assay according to the manufacturer's instructions (Promega, Madison, WI). Briefly, medium was aspirated, and a solution of 100 μL of F-12K containing 10% FBS and20 μL of a solution containing 4.76% phenazine methosulfate (PMS) in 3-(4,5-dimethylthiazol-2-yl)-5-(3-carboxymethoxyphenyl)-2-(4-sulfophenyl)-2H-tetrazolium, salt (MTS) was added into each well. Wells were scanned colorimetrically at 490 nm on a spectrophotometer after 150 min. The concentrations of free azBSA incubated with the HEK-293 cells (for 18 h) were equivalent to the level of azBSA attached to the particles in the cell viability studies presented in Figures 8 and 13. The conversion of MTS into an aqueous soluble formazan product is achieved only by dehydrogenase enzymes that are active in metabolizing cells; the absorbance at 490 nm from the formazan product is directly proportional to the number of living cells in culture. Cell viability was presented as percentage of viable cells in total population.

3. RESULTS AND DISCUSSION

A schematic of the particle-based system studied in this effort is presented in Figure 6. The poly(propargyl acrylate) (PA) colloids were prepared using an aqueous emulsion polymerization technique, which resulted in spheres with a diameter of ~88.5 nm. To functionalize the particle surface with the protein bovine serum albumin (BSA), BSA must be modified to have terminal azide groups. Standard BSA was reacted with excess azide-modified *N*-hydroxysuccinimide ester (azNHS) to produce azide-labeled BSA (azBSA) that has several free azide terminated groups. A multiple step CuAAC reaction was performed to conjugate alkyne terminated silicon phthalocyanine alSiPc to azBSA; then the PA particles were functionalized with the azBSA/alSiPc conjugate. Additionally, the alSiPc fluorophore can be replaced with an alkyne functionalized cyanine 3 dye (alCYN). With all dye systems, the intact particle−protein−dye constructs are not fluorescent; however, upon proteolytic digestion of azBSA, the system becomes fluorescence due to the release of the fluorophore. Furthermore, the dye on the particle−protein−dye system can be replaced with a targeting ligand, which will transition the system from passively targeting cancer cells to actively targeting cancer cells. All dyes and ligands utilized in this work are presented in Figure 7.

3.1. *In Vitro* Photodynamic Therapy Studies of Particle−Protein−Dye System. Our group previously reported on the synthesis and fluorescence imaging capabilities of PA particles modified with a shell of azide-modified BSA with a silicon phthalocyanine dye attached to the surface of the BSA shell (PA/azBSA/alSiPc). It was demonstrated that the system was environmentally responsive, and it was suggested that this system could be used for PDT. The following section confirms PDT activity of this PA/azBSA/alSiPc system.[25]

In PDT, upon excitation, the photosensitizer undergoes an intersystem crossing to longer-lived triplet states. This excited triplet-state energy is transferred to the ground-state triplet of the oxygen in tissue, and highly cytotoxic reactive singlet oxygen ($^1O_2$) is formed. This toxic singlet oxygen can directly kill tumor cells by inducing apoptosis or necrosis, result in the destruction of tumor vasculature, and can produce an acute inflammatory response that attracts leukocytes such as dendritic cells and neutrophils.[31]

DOI: 10.1021/acsabm.9b00025
ACS Appl. Bio Mater. XXXX, XXX, XXX−XXX

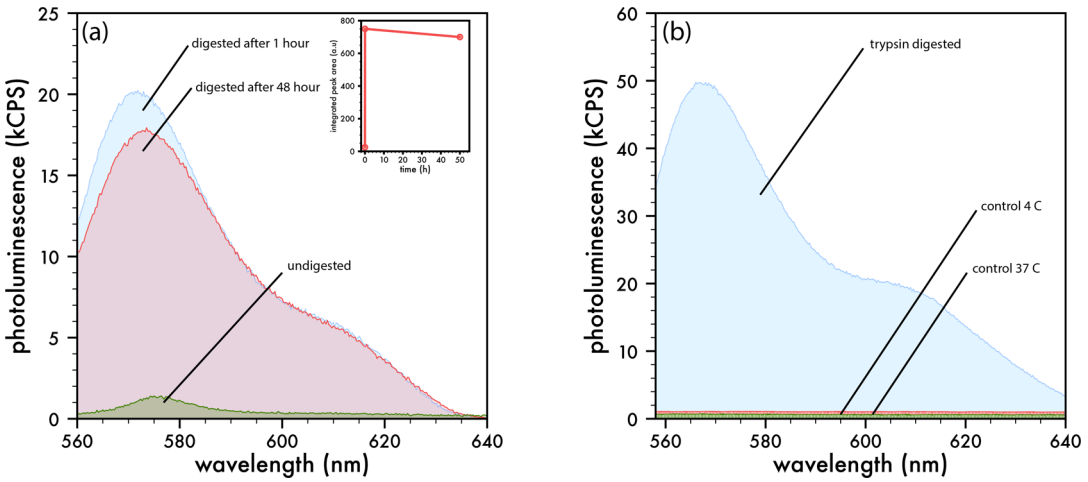

Figure 9. (a) Increase in photoluminescence intensity of PA/azBSA/alCYN nanoparticles with addition of trypsin and incubation for 1 and 48 h at 37 °C when dispersed in PBS. The inset presents the change in the integrated peak area of emission with the addition of trypsin. (b) Photoluminescence of the supernatants of the PA/azBSA/alCYN nanoparticles stored at 4 °C, incubated at 37 °C, and trypsin digested.

PDT studies (cf. Figure 8) with PA/azSiPc and PA/azBSA/alSiPc were performed. Here, the functionality of the fluorophore was changed to an alkyne to support the CuAAC reaction between the azide-modified BSA. Additionally, the fluorophore was changed from alSiPc to alSiPc2 to increase water solubility. In this PDT experiment, UMSCC22A cells were cultured for 24 h and then incubated with varying concentrations of PA/azSiPc or PA/azBSA/alSiPc2 for 18 h in culture medium. After 18 h, the cells were irradiated with 670 nm light, and cell death was assessed with propidium iodide exclusion over time. At all concentrations, PA/azBSA/alSiPc killed more cells than did PA/azSiPc. The optimal concentration of PA/azBSA/alSiPc to kill cells controllably was 1600 nM, which resulted in 12% cell death after 18 h. Without irradiating the PA/azBSA/alSiPc system, it showed no cytotoxicity (data not shown) toward the cells. This study confirmed that when particles are directly surface modified with fluorophores, the energy is lost, perhaps nonradiatively, and causes the singlet oxygen yields to diminish. It should be noted that the free fluorophores were confirmed to be toxic to cells by hour 10 (data not shown), while previous studies with similar PDT-enabled particles and no irradiation indicated no enhanced toxicity to the cells by the mere presence of the particles.[16]

3.2. Versatility of Particle−Protein−Dye System. As stated previously, the dye on the particle−protein−dye system can easily be changed. In this case, silicon phthalocyanine was replaced with a cyanine 3 (alCYN) derivative. An important feature of the PA/azBSA/alCYN nanoparticles is that the release of the free fluorophore upon tryptic digestion of the BSA still occurs. Initially, the modified particles have a decreased emission and are said to be in an emission "off" state because the fluorophore transfers energy non-radiatively to the protein and particle.[25] As with the PA/azBSA/alSiPc system, the protein acts as a linker that attaches the fluorophore to the particle, and it is expected that, digestion of the protein, which gets broken into smaller peptide chains, results in the release of the fluorophore. As the fluorophore is free and no longer attached to the particles, the non-radiative transfer of energy is decreased, which leads to a significant increase in the emission of the fluorophore. This emission activation is called the "on" state of the system. To illustrate the emission activation due to the release of the fluorophore from the modified particles, clean PA/azBSA/alCYN particles were incubated with 0.215 mM trypsin at 37 °C (cf. Figure 9a). After an hour of incubation, an increase of ∼2360% in integrated intensity area was observed, and that increase dropped slightly at longer incubation times. This response of the modified particles implied that the majority of the fluorophore was released within the first hour of incubation, and, at longer time periods, it is possible that the fluorophore is precipitating from solution or the emission is quenching due to aggregation of the fluorophores.[32,33] In addition, it can be argued that the emission "turn-on" of the modified particles could be from the denaturing of BSA. It is speculated that during the initial unfolding stage, emission could be activated due to the increased non-specific interaction between BSA and alCYN.[16] To disprove this speculation and confirm that the fluorophore was actually released, the PA/azBSA/alCYN particles were centrifuged at 15 000 rpm for 15 min to separate the particles from the free fluorophore. If the fluorophore was released, it would remain in the supernatant instead of remaining attached to the sediment (i.e., the particles), and measuring the emission of the supernatant of the trypsin digested particles would reveal whether the fluorophore was released. Figure 9b presents the emission of the supernatant when excited at 550 nm (i.e., maximum absorbance of alCYN). The undigested particles that were stored at 4 °C and the particles incubated at 37 °C without trypsin were used as controls in this supernatant study. For both controls, the supernatant obtained after centrifugation had no emission, and the supernatant of the trypsin digested particles had a strong emission (cf. Figure 9b). These measurements confirm the release of the fluorophore from the modified particles upon trypsin digestion. However, it is important to note that in some of the batches of the PA/azBSA/alCYN particles, the yields of the release of the fluorophore upon tryptic digestion were low. This inconsistency in the release of the fluorophore was anticipated and can be attributed to the modification of BSA and the digestion conditions.[34] In tryptic digestion, it is well established that trypsin cleaves at the amino side of the cysteine residues. The primary amines of the BSA are all modified for conjugation to azNHS to facilitate the attachment of the alCYN fluorophore,

DOI: 10.1021/acsabm.9b00025
ACS Appl. Bio Mater. XXXX, XXX, XXX−XXX

so there is a high possibility that most of the peptide bonds formed during the NHS coupling might not be cleavable by trypsin. Usually, the extent of digestion is defined by measuring the amino acid sequence coverage (SQ%), but this parameter can be an ambiguous measure since different mass spectrometers when coupled with different search parameters in subsequent data analysis may reveal a range of SQ% and is beyond the scope of this current project.[35,36] Instead of measuring the SQ%, a calorimetric study of thermal denaturation of the proteins was performed to understand the changes in the protein during the tryptic digestion. The nanoDSC curves obtained (cf. Figure 10) show the essential

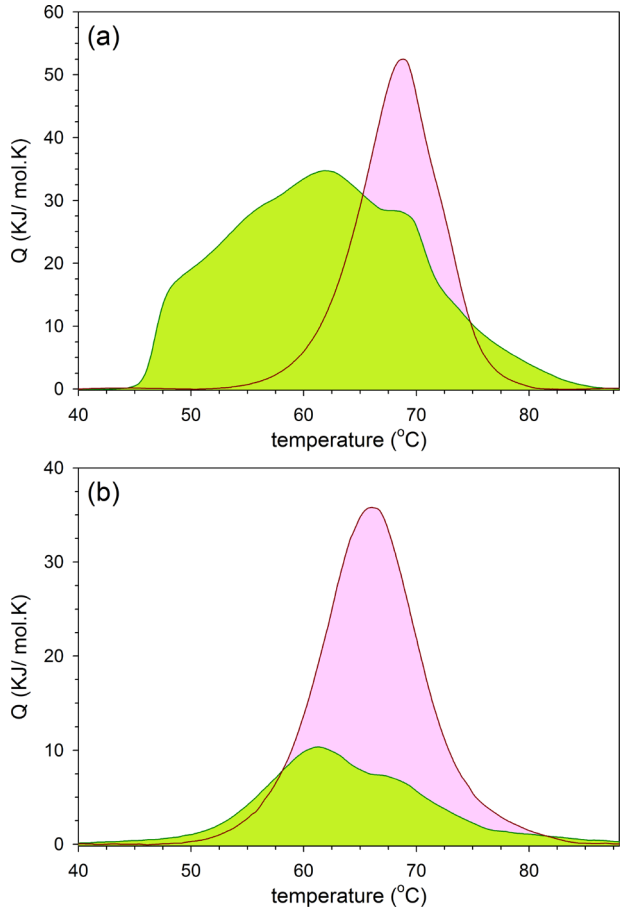

Figure 10. NanoDSC thermograms of (a) BSA and (b) azBSA. In both graphs, undigested proteins correspond to pink curves, and trypsin digested proteins correspond to green curves.

differences between the undigested and digested proteins. Both the undigested proteins exhibited a single endotherm peak in the nanoDSC curve. For the BSA curve, the single peak was near 69 °C, which agreed well will the data obtained from literature.[37] On the other hand, the azBSA curve showed a single peak near 66 °C, which indicated that there was a slight modification in the structure when compared to the native BSA but not a major conformation change. Regarding the digested proteins, instead of the single isothermal peak, multiple smaller peaks were observed in the nanoDSC curves. In those curves, the lower intensity of the peaks compared to undigested proteins indicated that most of the protein was denatured during the digestion step, and the multiple peaks obtained indicated that the changes observed could be from multiple structurally independent or dependent parts. Comparison of the data from the two digested proteins showed two main differences: (1) the onset temperature for denaturing the digested BSA was ∼44 °C, which was much lower compared to that of the digested azBSA; and (2) in the case of digested azBSA, there were two transitions, one at ∼62 °C and the other at ∼68 °C, whereas, for the digested BSA, apart from the two transitions at ∼62 °C and ∼68 °C, there were other additional transitions in the ∼44−60 °C temperature range. These differences in the calorimetric study confirm that the azBSA is not being completely digested by trypsin. This drawback of partial digestion of azBSA can be overcome by using other enzymes, such as pepsin, which have a higher digestion efficiency of serums than trypsin.[38] We mentioned earlier that apart from the modification of BSA, the digestion conditions could also lead to incomplete digestion of proteins. Usually to ensure a complete digestion of the protein, it is denatured prior to the digestion step because digestive enzymes, such as trypsin, cannot gain full access to the cleavage sites if the protein is folded or in the native globular form, and, upon denaturing the protein, the sites that were once inaccessible become available for cleaving. In general, the protein can be denatured in a number of ways including (1) high temperatures, (2) high/low pH (depending on the protein and enzyme), (3) change in ionic strength, and (4) addition of chaotropic agents and organic solvents.[39] In the above study, the PA/azBSA/alCYN particles were digested at 37 °C, which is lower than the irreversible unfolding temperature of BSA (i.e., 60−70 °C).[16] At 37 °C, there might be some unfolding, which is reversible so the trypsin can sometimes gain access to the cleavage sites, and this leads to low yields of the release of the alCYN from the modified particles. This issue can be corrected by denaturing the modified particles by one of the four methods mentioned above, prior to the tryptic digestion step. This sequential denaturation and digestion method will ensure a high release of the fluorophore, provided the right digestive enzyme is used.

3.2.1. Emission of Free alCYN and Interaction with Proteins. The absorbance and photoluminescence of alCYN when dispersed in a good solvent, such as methanol, are presented in Figure 11. In this solvent, alCYN has an absorbance maximum at 546 nm and the corresponding emission peak is at 569 nm, which gives a Stokes shift of 23 nm. alCYN exhibits a reduced emission when dispersed in aqueous solutions due to quenching of the dye because the dyes aggregate (cf. Figure 12a); however, for biological applications, the fluorophore must be dispersed in an aqueous solvent. These aggregates, upon excitation, transfer energy through a nonradiative pathway, which results in a vastly decreased emission of the fluorophore.[32,33] The emission of these large aggregates is typically activated by albumin proteins, which solubilize the fluorophore by breaking the aggregates and binding the fluorophore nonspecifically.[32,33] The activation of alCYN in a Tris-HCL buffer of pH 8 is presented in Figure 12a. Upon addition of 0.05 mM BSA to alCYN, a 4742% increase in the integrated peak area of the emission spectrum of alCYN was observed when comparing alCYN without BSA and alCYN after 1 h of BSA exposure. However, the activated emission can be deactivated using trypsin. It is well-known that trypsin digests BSA when incubated at high temperatures and at a pH of 7−8.[40,41] When ∼0.215 mM trypsin was added to the BSA/alCYN complex and incubated at 37 °C, BSA was digested into smaller

DOI: 10.1021/acsabm.9b00025
ACS Appl. Bio Mater. XXXX, XXX, XXX−XXX

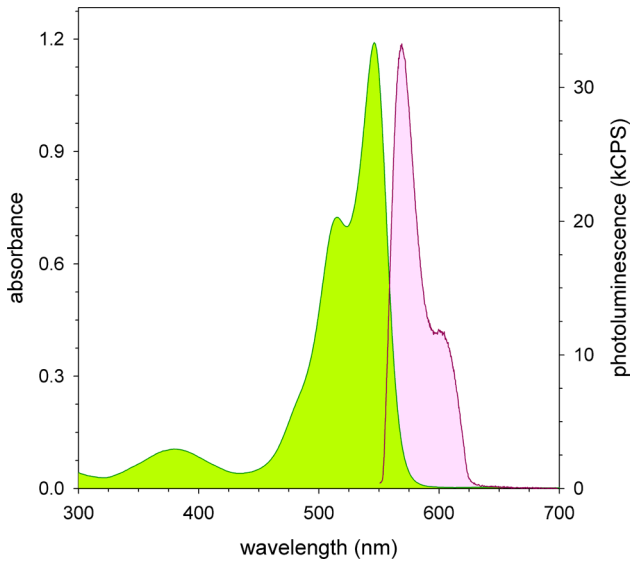

Figure 11. Absorbance (green) and photoluminescence (pink) of alkyne functionalized cyanine derivative fluorophore (alCYN; 12.21 μM in methanol).

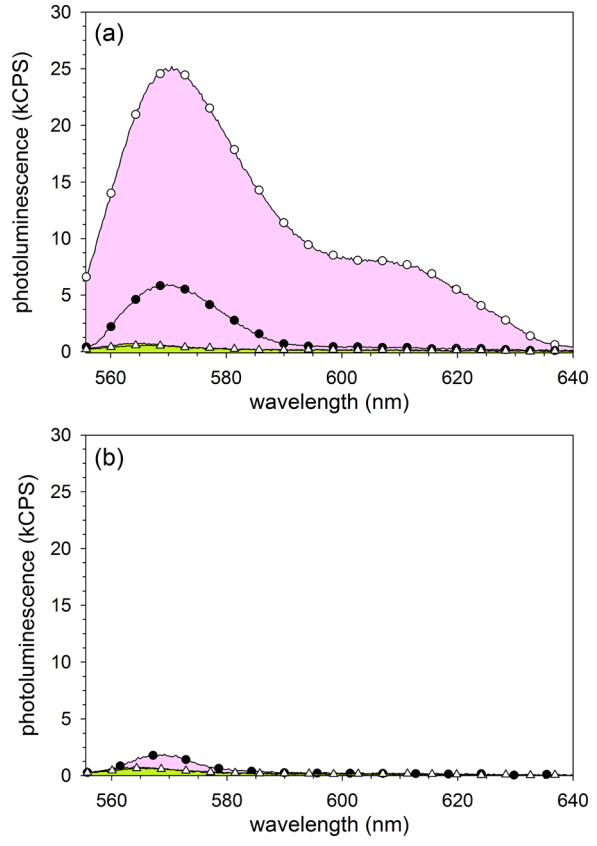

Figure 12. (a) Changes in photoluminescence intensity of (−) alkyne terminated cyanine fluorophore (alCYN), with addition of (○) ∼0.05 mM bovine serum albumin, followed by addition of ∼0.215 mM trypsin, and incubated for (●) 2 h and (Δ) 7203 h. (b) Changes in photoluminescence intensity of (−) alkyne terminated cyanine fluorophore (alCYN), with the addition of ∼0.215 mM trypsin, and incubated for (●) 2 h and (Δ) 7203 h.

peptides, which no longer bind to alCYN. This leads the alCYN to form aggregates and results in a quenched emission.

At longer periods of incubation of the albumin-activated alCYN with trypsin, the emission returned to the initial intensity as the BSA was completely digested. In addition to the activation/deactivation study of the alCYN, it is necessary to study the changes in emission of alCYN with trypsin to eliminate the possibility of trypsin activating the emission of alCYN. In this study, ∼0.215 mM trypsin was added to alCYN fluorophore and incubated at 37 °C. The emission of alCYN was monitored during incubation, and after 2 h of incubation, the photoluminescence intensity increased by 95% (cf. Figure 12b), which was much lower compared to the activation with albumin. After incubation for longer periods of time, the emission returned to the initial intensity as trypsin also digested itself. Therefore, from the activation studies of alCYN, it can be concluded that alCYN is selectively activated by BSA, and activation by trypsin is negligible in comparison to the activation by BSA.

3.3. Active Targeting of Particle−Protein−Ligand System. Apart from the delivery and therapy applications of the particle−protein−dye system, this multifunctional system can be expanded and used for active targeting applications by replacing the dye with a ligand that binds to a specific protein to enhance targeting capabilities of the ligand. For this enhanced targeting demonstration, the protein chosen is "Survivin", which is a member of the inhibitor of apoptosis (IAP) proteins and regulates cell division and death.[42,43] In addition, during fetal development in humans, Survivin is expressed but is rarely present in adult tissues, which makes it an attractive target for tumor theranostics in the medical community.[44−47] The ligand utilized was s102 (cf. Figure 7), which is an alkyne modified version of the original Abbott17 compound. In 2007, Abbott labs discovered a new direct binding site at the dimer interface of Survivin and a ligand, called Abbott17, which binds specifically to the dimer site using affinity-based screening methods.[27] In this current effort, the Abbott17 is modified to include an alkyne moiety (cf. Figure 7) to facilitate the conjugation to azBSA, and this small molecule ligand is referred to as s102. To determine the binding efficiency of the modified particles to Survivin and verify the enhancement in binding toxicity, studies were performed. The binding affinity between the protein and ligand is usually expressed by the binding dissociation constant, K_D, but in the case of the Survivin and Abbott17 binding, the binding efficiency is directly correlated to toxicity, so toxicity studies can be used to understand the binding efficiencies between them. The ligand binds to the dimer interface of the Survivin and blocks other proteins, such as Ran, which regulate the activity of Survivin. As these other apoptosis inhibitor proteins can no longer bind at the dimer interface, the Survivin cannot inhibit apoptosis, and cell death is observed.[48] Therefore, it can be concluded that higher binding of the ligand blocks the inhibitors binding at that site and leads to activation of apoptosis, which results in cell death, so cell toxicity is a direct indicator of the binding of the ligand to the protein. Toxicity studies were performed in A549 cells, which are known to overexpress Survivin. The A549 cells were treated with varying concentrations of s101, an azide-modified version of the Abbott17 compound (cf. Figure 7), and PA/azBSA/s102. After 48 h, the cell viability was determined using the MTS assay. From the cell viability data (cf. Figure 13), it is evident that the particles have a higher cell death, which indicates a higher binding affinity of the system compared to the free small molecule. This increase in cell death is as

DOI: 10.1021/acsabm.9b00025
ACS Appl. Bio Mater. XXXX, XXX, XXX−XXX

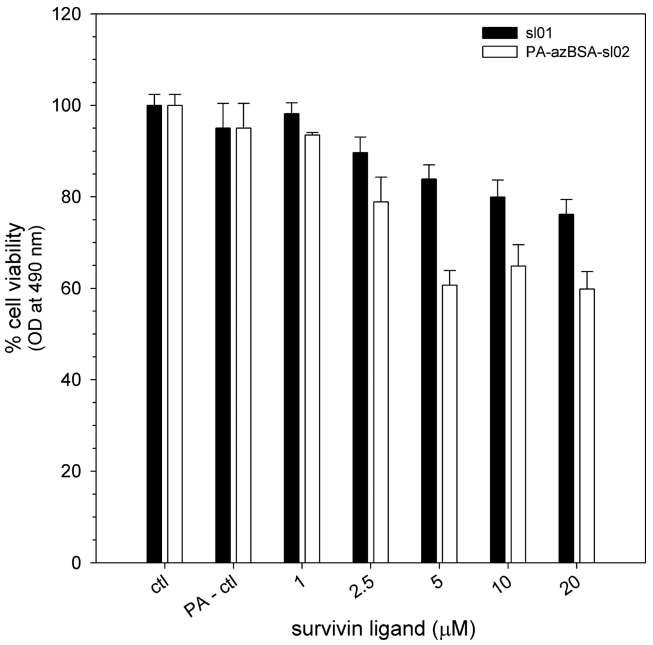

Figure 13. Cell viability data using the MTS assay with A549 cells. The cells were treated with s101 and PA/azBSA/s102 at varying concentrations for 48 h. Cell viability is presented as percentage of viable cells in total population.

expected because immobilizing the ligand on the particle increases the accumulation of the ligand inside the cells due to the enhanced permeation and retention effect,[49] and the higher accumulation leads to an increased blocking of the inhibitors that bind at the dimer interface, which results in enhanced cell death.

4. CONCLUSION

The sub 100 nm poly(propargyl acrylate) particles were surface modified with an azide-modified bovine serum albumin that is covalently conjugated to alkyne terminated fluorophore(s) through a multistep CuAAC reaction. Initially, these particles have a quenched emission, and upon trypsin digestion, they exhibited an activation of emission due to the cleavage of the protein and release of the fluorophore. This release strategy gave promising results when the silicon phthalocyanine fluorophore was used in photodynamic therapy studies. Additionally, the dye can be any alkyne-modified fluorophore as shown by replacing the silicon phthalocyanine with a cyanine 3 derivative, and the same fluorescence on/off behavior is observed. The dye could also be replaced with a targeting ligand, which can directly inhibit cancer growth, where the BSA now provides "stealth" to the particle. This versatile nanodevice is not just limited to the fight against cancer but has a huge potential to be expanded to treatment of several other diseases and vaccinations due to the ease of the modification of the particles with several moieties.

AUTHOR INFORMATION

Corresponding Author

*E-mail: foulger@clemson.edu.

ORCID

Stephen H. Foulger: 0000-0002-4221-2154

Notes

The authors declare no competing financial interest.

ACKNOWLEDGMENTS

The authors thank the Gregg-Graniteville Foundation and the National Science Foundation (OIA-1632881) for financial support as well as TA Instruments for use of the Nano DSC.

REFERENCES

(1) Yap, H. P.; Johnston, A. P. R.; Such, G. K.; Yan, Y.; Caruso, F. Click-engineered, bioresponsive, drug-loaded PEG spheres. *Adv. Mater.* **2009**, *21*, 4348.

(2) Sheng, Z. H.; Hu, D. H.; Xue, M. M.; He, M.; Gong, P.; Cai, L. T. Indocyanine Green nanoparticles for theranostic applications. *Nano-Micro Lett.* **2013**, *5*, 145−150.

(3) Lallana, E.; Fernandez-Trillo, F.; Sousa-Herves, A.; Riguera, R.; Fernandez-Megia, E. Click chemistry with polymers, dendrimers, and hydrogels for drug delivery. *Pharm. Res.* **2012**, *29*, 902−921.

(4) Riehemann, K.; Schneider, S. W.; Luger, T. A.; Godin, B.; Ferrari, M.; Fuchs, H. Nanomedicine-challenge and perspectives. *Angew. Chem., Int. Ed.* **2009**, *48*, 872−897.

(5) Sahoo, S. K.; Labhasetwar, V. Nanotech approaches to delivery and imaging drug. *Drug Discovery Today* **2003**, *8*, 1112−1120.

(6) Torchilin, V. P. Micellar nanocarriers: Pharmaceutical perspectives. *Pharm. Res.* **2006**, *24*, 1−16.

(7) Nasongkla, N.; Bey, E.; Ren, J. M.; Ai, H.; Khemtong, C.; Guthi, J. S.; Chin, S. F.; Sherry, A. D.; Boothman, D. A.; Gao, J. M. Multifunctional polymeric micelles as cancer-targeted, MRI-ultrasensitive drug delivery systems. *Nano Lett.* **2006**, *6*, 2427−2430.

(8) Le Droumaguet, B.; Nicolas, J.; Brambilla, D.; Mura, S.; Maksimenko, A.; De Kimpe, L.; Salvati, E.; Zona, C.; Airoldi, C.; Canovi, M.; Gobbi, M.; Noiray, M.; La Ferla, B.; Nicotra, F.; Scheper, W.; Flores, O.; Masserini, M.; Andrieux, K.; Couvreur, P. Versatile and efficient targeting using a single nanoparticulate platform: application to cancer and alzheimer's disease. *ACS Nano* **2012**, *6*, 5866−5879.

(9) Pokorski, J. K.; Breitenkamp, K.; Liepold, L. O.; Qazi, S.; Finn, M. G. Functional virus-based polymer-protein nanoparticles by atom transfer radical polymerization. *J. Am. Chem. Soc.* **2011**, *133*, 9242−9245.

(10) Cui, J. W.; Yan, Y.; Wang, Y. J.; Caruso, F. Templated Assembly of pH-labile polymerdrug particles for intracellular drug delivery. *Adv. Funct. Mater.* **2012**, *22*, 4718−4723.

(11) Cheng, Z. L.; Al Zaki, A.; Hui, J. Z.; Muzykantov, V. R.; Tsourkas, A. Multifunctional nanoparticles: Cost versus benefit of adding targeting and imaging capabilities. *Science* **2012**, *338*, 903−910.

(12) Torchilin, V. P. Multifunctional nanocarriers. *Adv. Drug Delivery Rev.* **2006**, *58*, 1532−1555.

(13) Dobrovolskaia, M. A.; McNeil, S. E. Immunological properties of engineered nanomaterials. *Nat. Nanotechnol.* **2007**, *2*, 469−478.

(14) Lallana, E.; Sousa-Herves, A.; Fernandez-Trillo, F.; Riguera, R.; Fernandez-Megia, E. Click chemistry for drug delivery nanosystems. *Pharm. Res.* **2012**, *29*, 1−34.

(15) Lallana, E.; Riguera, R.; Fernandez-Megia, E. Reliable and efficient procedures for the conjugation of biomolecules through Huisgen azide-alkyne cycloadditions. *Angew. Chem., Int. Ed.* **2011**, *50*, 8794−8804.

(16) Jetty, R.; Bandera, Y. P.; Daniele, M. A.; Hanor, D.; Hung, H. I.; Ramshesh, V.; Duperreault, M. F.; Nieminen, A. L.; Lemasters, J. J.; Foulger, S. H. Protein triggered fluorescence switching of near-infrared emitting nanoparticles for contrast-enhanced imaging. *J. Mater. Chem. B* **2013**, *1*, 4542−4554.

(17) Rungta, P.; Bandera, Y. P.; Roeder, R. D.; Li, Y. C.; Baldwin, W. S.; Sharma, D.; Sehorn, M. G.; Luzinov, I.; Foulger, S. H. Selective imaging and killing of cancer cells with protein-activated near-infrared fluorescing nanoparticles. *Macromol. Biosci.* **2011**, *11*, 927−937.

(18) Ju, S.; Yeo, W. S. Quantification of proteins on gold nanoparticles by combining MALDI-TOF MS and proteolysis. *Nanotechnology* **2012**, *23*, 1−7.

DOI: 10.1021/acsabm.9b00025
ACS Appl. Bio Mater. XXXX, XXX, XXX−XXX

(19) Seo, T. S.; Li, Z. M.; Ruparel, H.; Ju, J. Y. Click chemistry to construct fluorescent oligonucleotides for DNA sequencing. *J. Org. Chem.* **2003**, *68*, 609−612.
(20) Dirks, A. J. T.; van Berkel, S. S.; Hatzakis, N. S.; Opsteen, J. A.; van Delft, F. L.; Cornelissen, J.; Rowan, A. E.; van Hest, J. C. M.; Rutjes, F.; Nolte, R. J. M. Preparation of biohybrid amphiphiles via the copper catalysed Huisgen [3 + 2] dipolar cycloaddition reaction. *Chem. Commun.* **2005**, 4172−4174.
(21) Barber, D. M.; Sanganee, H. J.; Dixon, D. J. One-Pot Catalytic Enantioselective Synthesis of Tetrahydropyridines via a Nitro-Mannich/Hydroamination Cascade. *Org. Lett.* **2012**, *14*, 5290−5293.
(22) Cheng, X. Y.; Lowe, S. B.; Ciampi, S.; Magenau, A.; Gaus, K.; Reece, P. J.; Gooding, J. J. Versatile ″Click Chemistry″ Approach to Functionalizing Silicon Quantum Dots: Applications toward Fluorescent Cellular Imaging. *Langmuir* **2014**, *30*, 5209−5216.
(23) Wright, A. K.; Thompson, M. R. HYDRODYNAMIC STRUCTURE OF BOVINE. *Biophys. J.* **1975**, *15*, 137−141.
(24) Gu, J. M.; Anumala, U. R.; Lo Monte, F.; Kramer, T.; von Haussen, R. H.; Holzer, J.; Goetschy-Meyer, V.; Mall, G.; Hilger, I.; Czech, C.; Schmidt, B. 2-Styrylindolium based fluorescent probes visualize neurofibrillary tangles in Alzheimer's disease. *Bioorg. Med. Chem. Lett.* **2012**, *22*, 7667−7671.
(25) Burdette, M. K.; Jenkins, R.; Bandera, Y.; Powell, R. R.; Bruce, T. F.; Yang, X.; Wei, Y. Z.; Foulger, S. H. Bovine serum albumin coated nanoparticles for in vitro activated fluorescence. *Nanoscale* **2016**, *8*, 20066−20073.
(26) Rungta, P.; Bandera, Y. P.; Roeder, R. D.; Li, Y.; Baldwin, W. S.; Sharma, D.; Sehorn, M. G.; Luzinov, I.; Foulger, S. H. Selective Imaging and Killing of Cancer Cells with Protein-Activated Near-Infrared Fluorescing Nanoparticles. *Macromol. Biosci.* **2011**, *11*, 927−937.
(27) Wendt, M. D.; Sun, C. H.; Kunzer, A.; Sauer, D.; Sarris, K.; Hoff, E.; Yu, L. P.; Nettesheim, D. G.; Chen, J.; Jin, S.; Comess, K. M.; Fan, Y. H.; Anderson, S. N.; Isaac, B.; Olejniczak, E. T.; Hajduk, P. J.; Rosenberg, S. H.; Elmore, S. W. Discovery of a novel small molecule binding site of human Survivin. *Bioorg. Med. Chem. Lett.* **2007**, *17*, 3122−3129.
(28) Abadi, A. H.; Abouel-Ella, D. A.; Lehmann, J.; Tinsley, H. N.; Gary, B. D.; Piazza, G. A.; Abdel-Fattah, M. A. O. Discovery of colon tumor cell growth inhibitory agents through a combinatorial approach. *Eur. J. Med. Chem.* **2010**, *45*, 90−97.
(29) Abadi, A.; Al-Deeb, O.; Al-Afify, A.; El-Kashef, H. Synthesis of 4-alkyl (aryl)-6-aryl-3-cyano-2(1H)-pyridinones and their 2-imino isosteres as nonsteroidal cardiotonic agents. *Farmaco* **1999**, *54*, 195−201.
(30) Nieminen, A.-L.; Gores, G. J.; Bond, J. M.; Imberti, R.; Herman, B.; Lemasters, J. J. A novel cytotoxicity screening assay using a multiwell fluorescence scanner. *Toxicol. Appl. Pharmacol.* **1992**, *115*, 147−155.
(31) Castano, A. P.; Mroz, P.; Hamblin, M. R. Photodynamic therapy and anti-tumour immunity. *Nat. Rev. Cancer* **2006**, *6*, 535−545.
(32) Tong, H.; Hong, Y. N.; Dong, Y. Q.; Haussler, M.; Lam, J. W. Y.; Li, Z.; Guo, Z. F.; Guo, Z. H.; Tang, B. Z. Fluorescent ″light-up″ bioprobes based on tetraphenylethylene derivatives with aggregation-induced emission characteristics. *Chem. Commun.* **2006**, 3705−3707.
(33) Jisha, V. S.; Arun, K. T.; Hariharan, M.; Ramaiah, D. Site-selective binding and dual mode recognition of serum albumin by a squaraine dye. *J. Am. Chem. Soc.* **2006**, *128*, 6024−6025.
(34) Butler, J. E. Solid supports in enzyme-linked immunosorbent assay and other solidphase immunoassays. *Methods* **2000**, *22*, 4−23.
(35) Xu, F.; Wang, W. H.; Tan, Y. J.; Bruening, M. L. Facile Trypsin immobilization in polymeric membranes for rapid, efficient protein digestion. *Anal. Chem.* **2010**, *82*, 10045−10051.
(36) Kolsrud, H.; Malerod, H.; Ray, S.; Reubsaet, L.; Lundanes, E.; Greibrokk, T. A critical review of trypsin digestion for LC-MS based proteomics. *Integrative Proteomics* **2012**, 73.
(37) Michnik, A. Thermal stability of bovine serum albumin DSC study. *J. Therm. Anal. Calorim.* **2003**, *71*, 509−519.
(38) Jones, R. G. A.; Landon, J. Enhanced pepsin digestion: a novel process for purifying antibody F(ab ')(2) fragments in high yield from serum. *J. Immunol. Methods* **2002**, *263*, 57−74.
(39) Proc, J. L.; Kuzyk, M. A.; Hardie, D. B.; Yang, J.; Smith, D. S.; Jackson, A. M.; Parker, C. E.; Borchers, C. H. A quantitative study of the effects of chaotropic agents, surfactants, and solvents on the digestion efficiency of human plasma proteins by Trypsin. *J. Proteome Res.* **2010**, *9*, 5422−5437.
(40) Lopez-Ferrer, D.; Capelo, J. L.; Vazquez, J. Ultra fast trypsin digestion of proteins by high intensity focused ultrasound. *J. Proteome Res.* **2005**, *4*, 1569−1574.
(41) Capelo, J. L.; Carreira, R.; Diniz, M.; Fernandes, L.; Galesio, M.; Lodeiro, C.; Santos, H. M.; Vale, G. Overview on modern approaches to speed up protein identification workflows relying on enzymatic cleavage and mass spectrometry-based techniques. *Anal. Chim. Acta* **2009**, *650*, 151−159.
(42) Chettiar, S. N.; Cooley, J. V.; Park, I. H.; Bhasin, D.; Chakravarti, A.; Li, P. K.; Li, C. L.; Jacob, N. K. Design, synthesis and biological studies of Survivin Dimerization Modulators that prolong mitotic cycle. *Bioorg. Med. Chem. Lett.* **2013**, *23*, 5429−5433.
(43) Li, F. Z.; Ambrosini, G.; Chu, E. Y.; Plescia, J.; Tognin, S.; Marchisio, P. C.; Altieri, D. C. Control of apoptosis and mitotic spindle checkpoint by Survivin. *Nature* **1998**, *396*, 580−584.
(44) Altieri, D. C. Validating Survivin as a cancer therapeutic target. *Nat. Rev. Cancer* **2003**, *3*, 46−54.
(45) Altieri, D. C. Survivin, versatile modulation of cell division and apoptosis in cancer. *Oncogene* **2003**, *22*, 8581−8589.
(46) Ambrosini, G.; Adida, C.; Altieri, D. C. A novel anti-apoptosis gene, survivin, expressed in cancer and lymphoma. *Nat. Med.* **1997**, *3*, 917−921.
(47) Fukuda, S.; Pelus, L. M. Survivin, a cancer target with an emerging role in normal adult tissues. *Mol. Cancer Ther.* **2006**, *5*, 1087−1098.
(48) Guvenc, H.; Pavlyukov, M. S.; Joshi, K.; Kurt, H.; Banasavadi-Siddegowda, Y. K.; Mao, P.; Hong, C.; Yamada, R.; Kwon, C. H.; Bhasin, D.; Chettiar, S.; Kitange, G.; Park, I. H.; Sarkaria, J. N.; Li, C. L.; Shakhparonov, M. I.; Nakano, I. Impairment of Glioma stem cell survival and growth by a novel inhibitor for survivin-ran protein complex. *Clin. Cancer Res.* **2013**, *19*, 631−642.
(49) Maeda, H.; Wu, J.; Sawa, T.; Matsumura, Y.; Hori, K. Tumor vascular permeability and the EPR effect in macromolecular therapeutics: a review. *J. Controlled Release* **2000**, *65*, 271−284.

DOI: 10.1021/acsabm.9b00025
ACS Appl. Bio Mater. XXXX, XXX, XXX−XXX